Available online at www.sciencedirect.com
ScienceDirect
Energy Reports 8 (2022) 149–158
www.elsevier.com/locate/egyr

2021 7th International Conference on Advances in Energy Resources and Environment Engineering (ICAESEE 2021), November 19–21, 2021, Guangzhou, China

Wave energy assessment for the nearshore region of the northern South China Sea based on in situ observations

Wuyang Chen[a,b,c,1], Junliang Liu[a,b,1], Junmin Li[a,b,e,*], Lu Sun[d], Bo Li[a,b,e], Huanlin Xing[b], Ping Shi[a,b]

[a] *Southern Marine Science and Engineering Guangdong Laboratory (Guangzhou), Guangzhou 511458, China*
[b] *State Key Laboratory of Tropical Oceanography, Key Laboratory of Science and Technology on Operational Oceanography, Guangdong Provincial Observation and Research Station for Coastal Upwelling Ecosystem, South China Sea Institute of Oceanology, Chinese Academy of Sciences, Guangzhou 511458, China*
[c] *School of Electronics and Information Engineering, Guangdong Ocean University, Zhanjiang 524025, China*
[d] *South China Sea Environmental Monitoring Center, State Oceanic Administration, Guangzhou 510300, China*
[e] *Sanya Institute of Oceanology, South China Sea Institute of Oceanology, Chinese Academy of Sciences, Sanya 572025, China*

Received 9 February 2022; accepted 8 March 2022
Available online xxxx

Abstract

The northern coastal region of the South China Sea (SCS) is the key area for wave energy research and application. Planning for wave energy resources and equipment development depends on the accurate assessment of energy distribution and variation characteristics. Based on in situ observation data for 19 months, this paper systematically assesses the wave energy resources of three typical coastal sites in the northern SCS. The results show that wave energy resources have significant temporal and spatial variabilities. The eastern part of the SCS's northern shore has the most energy, followed by the western part and the center part. The mean energy densities during the observation period are 2.1, 0.75, and 0.33 kW/m, respectively. The energy density is relatively high in summer, followed by winter and autumn, and relatively low in spring. For example, the mean energy densities on the northeast coast of the SCS in the four seasons are 3.1, 1.8, 1.7, and 1.2 kW/m, respectively. Based on statistics for three in situ sites, the considerable energy is mostly contributed by the sea state with a wave height between 0.5 m and 1.5 m and a period between 5 s and 9 s. This study emphasizes the importance of in situ observations for wave energy measurement in nearshore locations, and the results may provide support for the planning and utilization of wave energy in the northern SCS.

Peer-review under responsibility of the scientific committee of the International Conference on Advances in Energy Resources and Environment Engineering, ICAESEE, 2021.

Keywords: Wave energy; In situ observation; Energy assessment; Nearshore area; The South China Sea

* Correspondence to: State Key Laboratory of Tropical Oceanography, South China Sea Institute of Oceanology, Chinese Academy of Sciences, Guangzhou 511458, China.
E-mail address: jli@scsio.ac.cn (J. Li).
[1] The authors contributed equally to this work.

https://doi.org/10.1016/j.egyr.2022.03.068

Peer-review under responsibility of the scientific committee of the International Conference on Advances in Energy Resources and Environment Engineering, ICAESEE, 2021.

1. Introduction

Ocean wave energy has the advantages of green, clean, sustainable utilization, and great development potential. It is implemented as a strategic resource in the world [1,2]. With technological progress of the energy collection equipment, the economic competitiveness of wave energy will continue to increase, which has great development value and application prospects [3,4]. For offshore projects with high power grid construction costs, such as marine ranches, observation equipment, and drilling platforms, wave energy can effectively provide flexible and low-cost power guarantees.

The nearshore region of the northern South China Sea (NSCS) has frequent global economic activities and is also the priority area for marine resource development and utilization. The region has many marine ranches and marine power test sites. It is important to objectively assess the wave energy resources in response to the technical development and application needs of power generation [4–6].

At present, many studies have contributed efforts to the evaluation of wave power of the South China Sea (SCS). Since data from long time series are required, the data used for wave energy calculation are generally based on the results of numerical models. Many mature numerical models, such as Simulating Waves Nearshore and Wave Watch III, were applied to wave energy assessments (e.g., [7–10]). However, most of the existing researches mainly emphasized their results on the whole SCS and other open sea areas; for coastal waters, numerical models often cannot directly provide reliable calculation results. This is because coastal waters are more affected by terrain and other factors, and the resolution of general numerical models has difficulty effectively describing the impact of coastal terrain on waves [10–12]. Although several studies have assessed wave energy resources by deploying observation equipment and using field-measured wave data in the NSCS [6,13], most of the reported evaluation studies are for a local sea area, while there are still few studies on simultaneous monitoring for different regions in the NSCS.

In this study, typical stations were established in the NSCS's eastern, middle, and western coastal zones to carry out long-term series observations of wave parameters (Fig. 1). Based on field observation data, the reserves, stability, and seasonal differences in wave energy resources in the NSCS's coastal areas are systematically assessed. In addition, by comparing with the evaluation results of model reanalysis data, the importance of using observation data for nearshore wave energy evaluation is discussed.

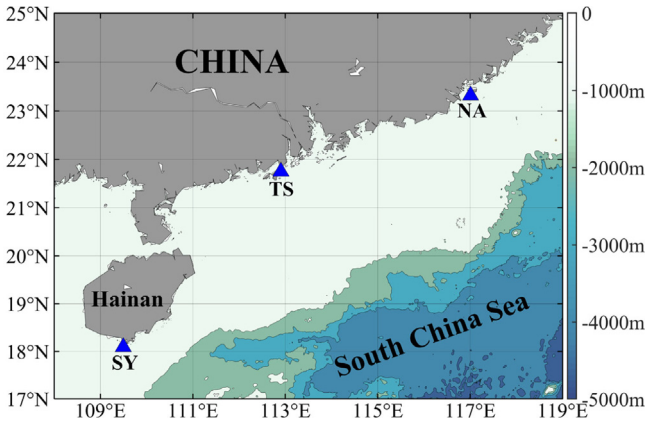

Fig. 1. Locations of study sites; the color indicates topography; the abbreviations "SY" stand for Sanya, "TS" for Taishan, and "NA" for Nan-ao. (For interpretation of the references to color in this figure legend, the reader is referred to the web version of this article.)

2. Data and methods

2.1. In situ observations

In this study, three nearshore observation sites are set in the SCS's north coast, in the west, middle, and east (Fig. 1). Among them, the western site "SY" is located to the southwest Luhuitou Peninsula, Sanya City, Hainan Province (18.1°N, 109.5°E), the middle site "TS" is located in the south nearshore area of Taishan City, Guangdong

Province (21.7°N, 112.9°E), and the eastern site "NA" is located in Shantou City, Guangdong Province, to the south of Nan-ao Island (23.3°N, 117.0°E). The distances from the three sites to the shores are approximately 300 m. The water depths of the SY, TS and NA sites are 14.1 m, 4.6 m, and 9.8 m, respectively.

Nortek acoustic wave and current profiler (AWAC) is used as the observation equipment at each study site. By placing the AWAC at the sea bottom and using the surface acoustic tracing method, wave samples are observed and collected upward. In this study, each sampling of AWAC lasted for 17 min with 2048 wave surface samples obtained, and each sampling interval was 0.5 h. Through spectral analysis of the wave surface samples, wave parameters including as significant wave height (Hs), main direction (Dp), and spectrum peak period (T_P) were obtained. The AWAC is connected to a shore platform through a cable, and the shore platform generates power for the AWAC through solar power. The shore-based platform transmits the observation data back to the laboratory in real-time through a GPRS signal. Similar observation sites have been deployed in different nearshore regions in the SCS [14,15].

The observation period in this study ranged from April 15, 2020, to November 30, 2021, and lasted for 19 months. The SY site has been deployed since April 2020, cable failure occurred in October 2020, was repaired in May 2021, and continues to operate until now. The TS site was deployed from July 2020 until July 2021. The NA site has been deployed since October 2020, overturned in equipment posture in May 2021, repaired in June 2021, and has been in operation ever since. All three sites were run for more than one year.

2.2. Model reanalysis data

To verify the importance of the in situ observations to the estimation of wave energy for nearshore regions, the output data produced by numerical models at the same periods as the in situ observation is employed. The calculation results of the model data are compared with those based on the in situ observations. The ERA5 model reanalysis data is employed in this study. The data is produced by the European Centre for Medium-Range Weather Forecasts, distributed by the Copernicus Climate Data Store, and have been applied for multiple studies regarding wave energy assessment (e.g., [2]). The calculation periods of the model data for the sites are the same as those of the observation periods.

2.3. Assessment method of wave energy resources

According to the estimation algorithms proposed by previous studies [13,16], the energy density and period of the waves are computed by:

$$Pw = 0.42Hs^2Tp \tag{1}$$

$$Te = \alpha Tp \tag{2}$$

where Pw and Te are the energy density (kW/m) and the energy period (s), respectively; α is an empirical coefficient which is decided by the wave spectrum to determine the sea condition. We used a cautious approximation of 0.9 [17] in this study.

Because stable wave energy is advantageous to energy acquisition and energy conversion, it is critical to assess the stability for the design and development of wave energy converters (WECs) [17]. The coefficient of variation (Cv) is applied to quantify the stability by the formula [18]:

$$Cv = \sqrt{\sum_{i=1}^{N} \left(Pw_i - \overline{Pw}\right)^2 / N} / \overline{Pw} \tag{3}$$

where N is the sample size of Pw.

The available level frequency (ALF) and the rich level frequency (RLF) are significant indicators for determining how rich wave energy resources are. According to the analysis results of [19,20], ALF and RLF are defined as follows:

$$F = n\left(Pw \geq t, 0.5\ \text{m} \leq Hs \leq 4\ \text{m}\right)/N \times 100\% \tag{4}$$

where s is the threshold value that $t = 2$ kW/m for $F =$ ALF and $t = 20$ kW/m for $F =$ RLF, and n is the sample size in which Pw and Hs meet the appropriate conditions.

3. Results and discussion

3.1. Statistical characteristics of wave energy

The observation results of the wave parameters (*Hs*, *Tp*, and *Dp*) and the calculation results of wave energy density (*Pw*) at three stations are shown in Fig. 2. The wave energy roses at the sites can be obtained by further statistics on the directional distribution of *Pw* (Fig. 3). The results show that the waves at the sites show typical characteristics of nearshore waves. The waves mainly propagate from the open sea toward the shore, with the direction relatively concentrated to shoreward. Due to the shallow effect of nearshore topography [21,22], *Hs* is mostly below 1.5 m, and *Tp* is mostly below 10 s. Accordingly, *Pw* is below 5 kW/m most of the time. By comparing the three sites, it can be found that the *Hs* and *Pw* of the NA site in the east are generally greater than those of the other two sites, followed by the SY site and the TS site. The mean *Pw* of the NA, SY, and TS sites in the observation period was 2.1, 0.75, and 0.33 kW/m, respectively.

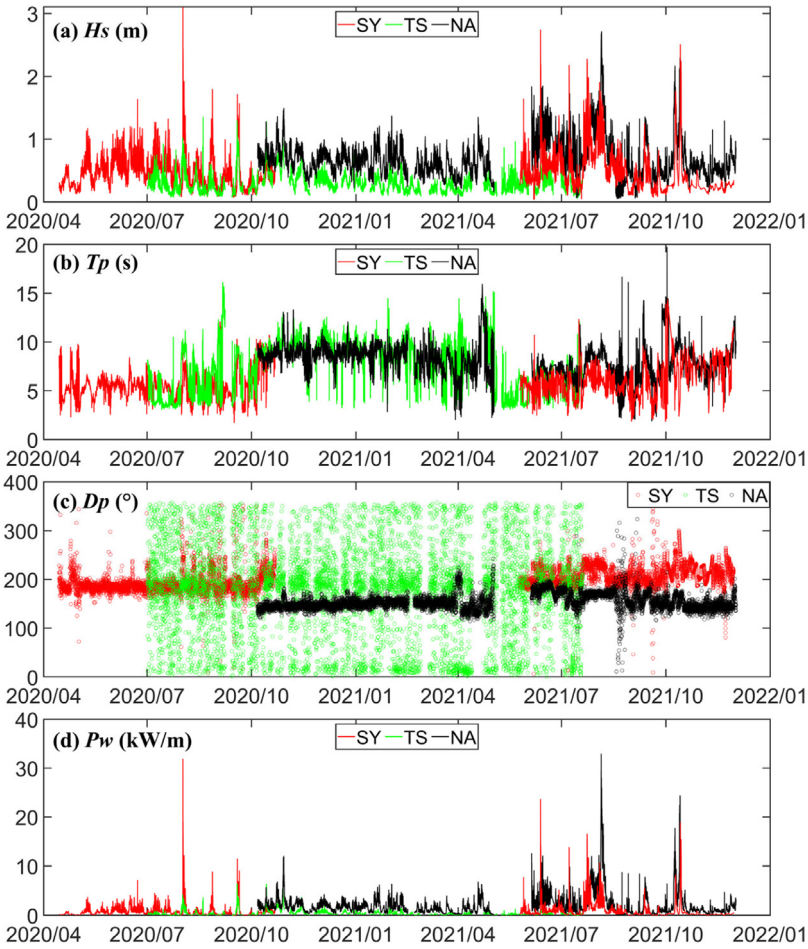

Fig. 2. Observational series of significant wave height (*Hs*), main direction (*Dp*), spectrum peak period (*Tp*), and calculation results of the wave energy density (*Pw*) at the three sites.

The difference in *Pw* among the three sites is related to the weakening effect of shallow topography [21,22] on the wave propagation path. Previous studies have shown that the waves in the NSCS mainly come from the Luzon Strait in the east and propagate along the southwest by west direction [23]. In the nearshore area, the waves are affected by the shoreline and underwater topography, deflect to the north, and gradually change into shoreline propagation [23,24]. By comparing the terrain in the NSCS, the location of the sites (Fig. 1), and the source direction

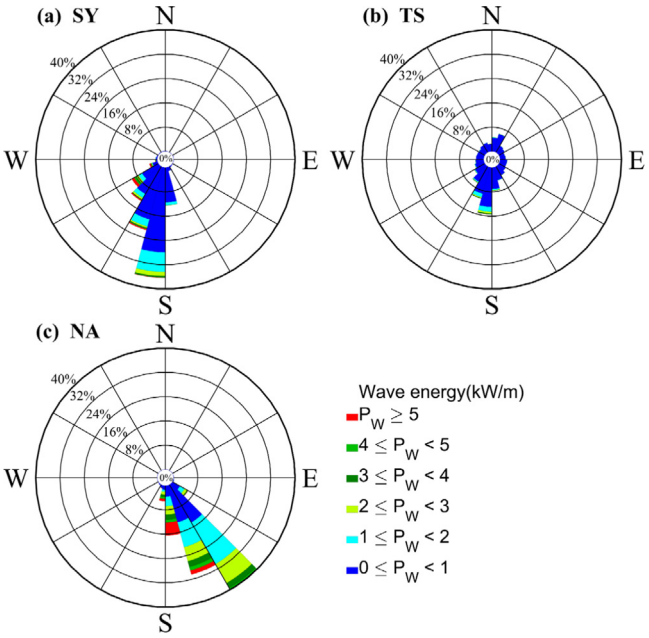

Fig. 3. Wave energy roses at the three sites.

of wave energy (Fig. 3), it can be found that the southeast of the NA site faces the near open ocean, and the waves arrive at the station shortly after they enter the NSCS from the Luzon Strait. Therefore, the waves are less affected by the reduction in shallow water topography than the other two sites. The TS site has the shallowest water depth among the three sites. Due to the long-distance shallow waters of the continental shelf that need to pass from the deep sea to this area, the wave energy at the site is weakened to the highest extent. Although the SY site is far from the Luzon Strait, the propagation process of the waves is mainly experienced in the deep-sea region in the NSCS. Waves do not deflect to the north until approximately 18°N and 110°E, which is affected by shallow water topography. Therefore, the wave energy in this area is still higher than that at the TS site. Previous observational studies have also shown that the *Pw* in the coastal region of Shenzhen, located in the middle of the north coast of the SCS, is also low [13].

Clarifying the contribution of different sea states under certain *Hs* and *Te* on the total *Pw* is critical for WECs' design (e.g., [8–10,13]). Our results show that the sea states contributing most to the wave energy are different for SY, TS, and NA sites (Fig. 4). According to the observation results of SY sites, the wave energy in the west coastal NSCS is mainly concentrated under conditions with a *Te* of 3–4 s and a *Hs* of 0.5–1.0 m. The results of the TS site show that in the middle nearshore region, the wave energy is mainly contributed by the sea conditions with a *Te* of 4–6 s and a *Hs* of less than 1.0 m. Observations at the NA site show that the wave energy is mainly concentrated under conditions with a *Te* of 4–5 s and a *Hs* of 0.5–1.0 m in the eastern nearshore NSCS. The results may supply a basic parameter reference for the WEC designs in similar regions.

3.2. Seasonal variations of wave energy

The surface wind field of the SCS is dominated by monsoons [25], with strong northeasterly winds in winter (December to February), southwesterly winds in summer (June to August), and relatively weak winds during monsoon transition periods in spring (March to May) and autumn (September to November). Correspondingly, waves and wave energy also show seasonal variations [16,26]. Therefore, based on the observed data at three sites, the data are further divided by seasons to estimate the seasonal variations of the energy in the NSCS (Figs. 5–7). The analysis results show that the seasonal differences of the three sites are consistent. As shown in Fig. 5, the *Pw*, ALF, and RLF of the sites are relatively high in summer, which is followed by winter and autumn seasons, and are

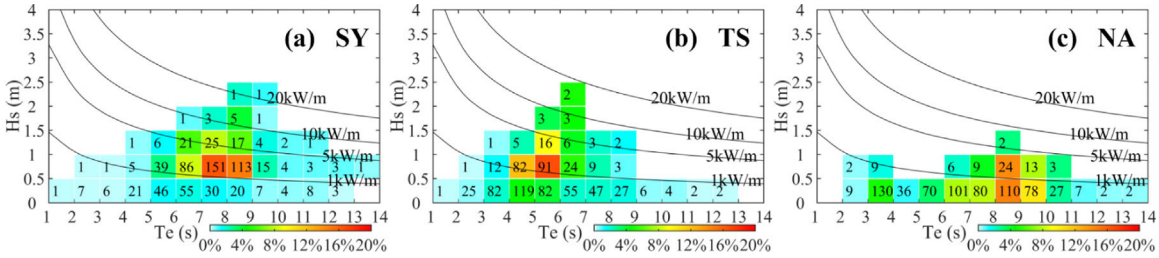

Fig. 4. Distributions of *Pw* contribution under different sea states represented by *Te* and *Hs* averaged over the observation periods at the three sites; the color represents the *Pw* contribution in certain *Hs* and *Te* combinations in a unit of percentage, the numbers mark the occurrence times of certain *Hs* and *Te* combinations in a unit of hours per month, and the isolines indicate the *Pw* calculated by Eq. (1).

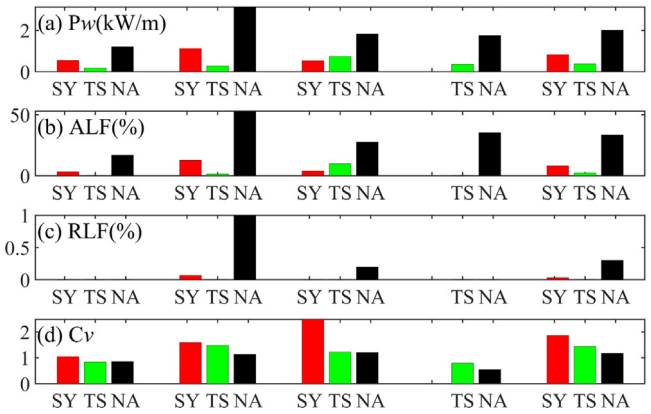

Fig. 5. Average values of *Pw*, ALF, RLF, and *Cv* in the four seasons and throughout the year at the three sites.

relatively low in spring. The stability difference is not obvious among seasons. Except for the SY site in autumn, the *Cv* values fluctuate by approximately 1.

The results indicate that the seasonal variations of wave energy are mainly influenced by both monsoon and coastal factors. Because local waves are influenced by swells propagating from the deep sea [24], the wave intensity is related to the basin-scale wind field in the SCS. During the summer monsoon, waves generated by southwesterly wind mainly propagate northward [16,26], and the waves reaching the sites are not blocked by the continental shoreline (Fig. 6b); thus, wave energy resources are relatively more abundant. However, the waves generated by the winter monsoon mainly propagate to the south. These waves are diffracted by shallow water topography and then spread northwest to reach the nearshore sites (Fig. 6d). These waves have a path to be shallowed by topography and refractive effects, making the wave energy remarkably lower than that during the summer monsoon. Spring and autumn are in the monsoon transition period, so the coastal waves in the NSCS may come from the south or southeast (Fig. 6a, c). Compared with spring, the monsoon transition period in autumn is relatively short, and the wind speed is relatively high. Accordingly, the wave energy in the coastal SCS is able to maintain relative high levels in autumn, compared to the situation in spring.

Further analysis of the wave energy distribution under different sea conditions shows that the contribution of wave energy under different *Hs* and *Te* is different in the four seasons. As shown in Fig. 7, in summer, wave energy is mainly concentrated in wave with 0.5–1.5 m *Hs*, while in other seasons, wave energy is mainly concentrated in waves with 0.5–1.0 m *Hs*. On the other hand, the wave energy in spring and summer mainly concentrates on the wave with a *Te* of 5–8 s, while in autumn and winter, the wave energy concentrates on the wave for a relatively long period (7–9 s). Therefore, when designing WECs, more flexible design schemes should be adopted if possible to meet the operational requirements of different sea conditions.

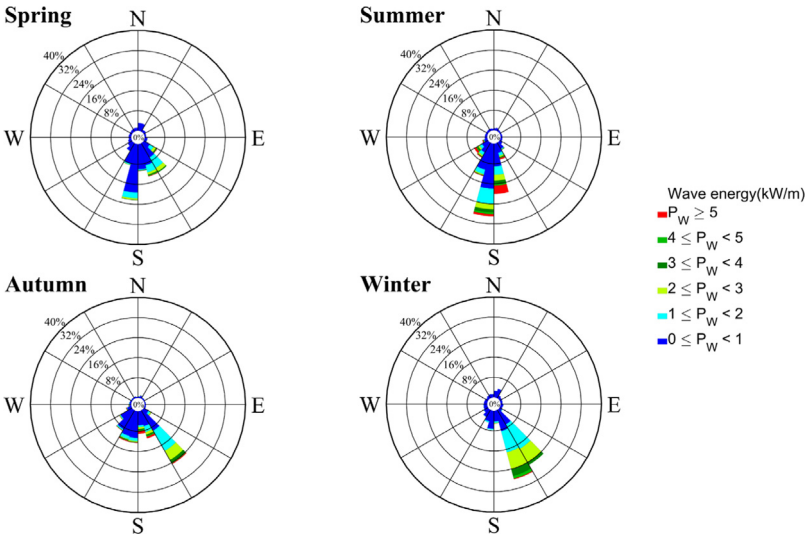

Fig. 6. Wave energy roses in the four seasons average over the three sites.

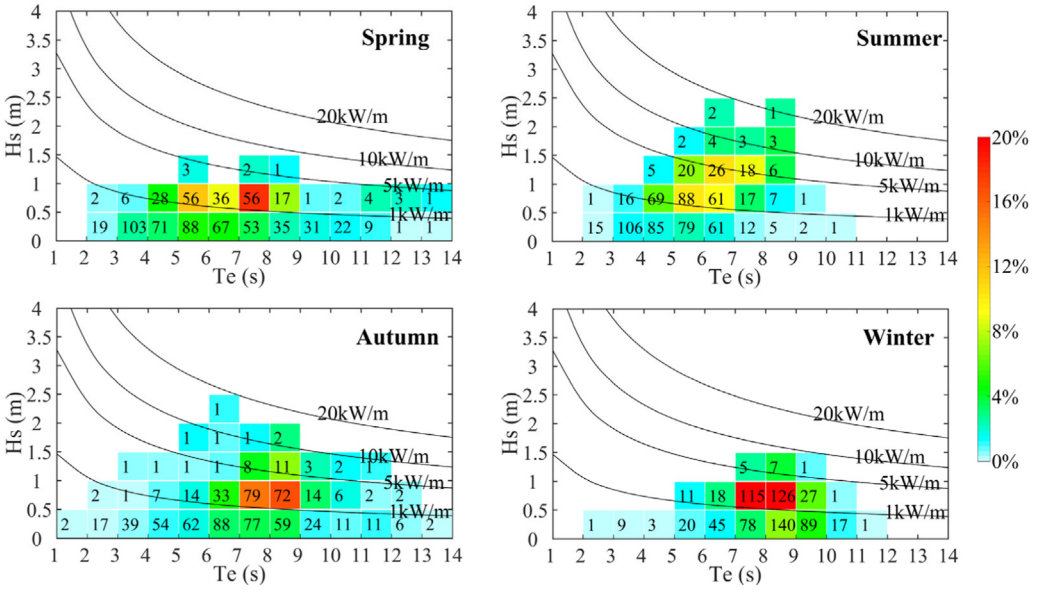

Fig. 7. Similar to Fig. 4 but for the four seasons averaged over the three sites.

3.3. Comparison with the assessment based on model data

To verify the importance of field observation data for the wave energy assessment in nearshore regions, the above wave power calculations were redone using ERA5 model reanalysis data. The results indicate that the assessment may be larger than the actual situation if it is based on model outputs (Fig. 8), which may lead to a waste of wave energy development. This inaccuracy may be due to the inadequacy of the numerical model in grid resolution, topographic information, and computing resources, which makes it difficult to accurately describe the wave dynamic process under shallow topography [11,12]. For example, waves in nearshore regions not only include swells that come from the open sea but also include local waves affected by surface wind and underwater topography; thus, the *Pw* in nearshore regions is generally less than that in offshore regions [27]. Such differences require high-resolution numerical models with enough characterization capability for complicated wave dynamics [9,10].

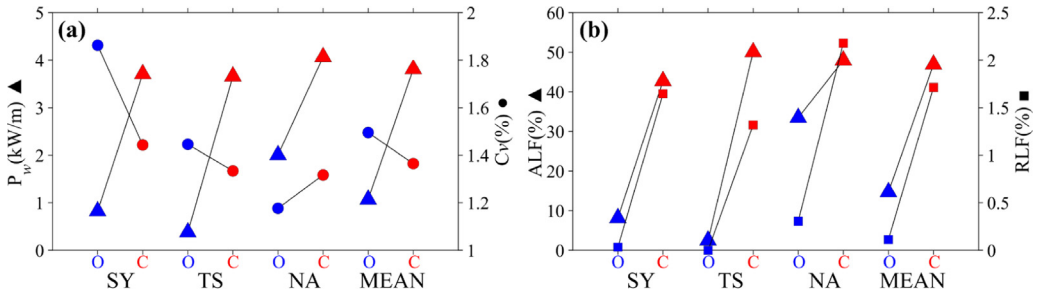

Fig. 8. Comparison of wave energy parameters calculated by in situ observations (plots in blue) and by ERA5 model data (plots in red); (a) is the annual and seasonal mean of *Pw* and *Cv*, and (b) is the annual and seasonal mean of ALF and RLF.

Although several numerical models have been established specifically for local regions (e.g., [7,28]), the accuracy of several models is still insufficient for relatively nearshore regions compared to the open sea region. It is necessary to calibrate the model results for nearshore regions based on in situ observations before they are used for wave energy assessments [11,28,29].

Moreover, the main energy distribution in different *Te* and *Hs* may be misjudged, if the model data are applied to calculate the sea state contributions (Fig. 9). For example, the main energy contribution calculated by observed data is provided by the sea state with 0.5–1 m *Hs* and 7–9 s *Te*. However, if the calculation is based on the model data, the results show that the wave energy is mainly distributed at sea state with 1.5–2.5 m *Hs* and 6–8 s *Te*. Therefore, assessments based on model data may underestimate the contribution of waves with lower wave heights and longer energy cycles. Incorrect energy distribution results may further mislead the designs of WECs.

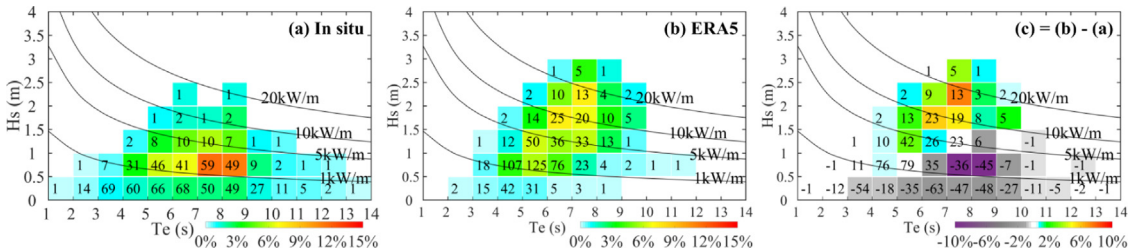

Fig. 9. Similar to Fig. 4 but for the average over the three sites and the four seasons, based on (a) in situ data, (b) ERA5 model data, and (c) their difference (i.e., (b) minus (a)).

4. Conclusions

The wave energy resources in the northern coastal regions of the South China Sea were systematically assessed using field observation data from three typical sites with a period of 19 months. The wave energy resources at the Nan-ao site in the east nearshore region are relatively high, followed by the Sanya site in the west nearshore region and the Taishan site in the middle nearshore region. Their average wave energy densities during the observation period are 2.1, 0.75, and 0.33 kW/m, respectively. The resources in the region are affected by the monsoon and local topography, showing obvious seasonal variation characteristics. The energy density is relatively high in summer, low in spring, and moderate in winter and autumn. The energy is mainly contributed by the sea state with 0.5–1.5 m significant wave height throughout the year. The energy is mainly distributed in the energy period of 5–8 s during spring and summer, while in the period of 7–9 s during winter and autumn. Further analysis shows that if the wave energy assessment is based on model data in the nearshore region, it may overestimate the wave energy density or misjudge the main sea state contributions most to the total wave energy, resulting in a waste of development cost, or the designed device cannot reach the optimal performance. These results may provide reference knowledge and technical parameters to support the wave energy planning and development in the region.

Declaration of competing interest

The authors declare that they have no known competing financial interests or personal relationships that could have appeared to influence the work reported in this paper.

Acknowledgments

The deployments of the hydrological monitoring platforms were supported by Shantou Station and Nan-ao Station, China, Shanwei Marine Environment Monitoring Center, China, State Oceanic Administration, China. The analysis in this study is supported by the High-Performance Computing Division in the South China Sea Institute of Oceanology. This study is supported by the Key Special Project for Introduced Talents Team of Southern Marine Science, China and Engineering Guangdong Laboratory (Guangzhou), China (GML2019ZD0302), the Science and Technology Projects of Guangdong Province, China (2021B1212050023), National Natural Science Foundation of China, China (41776005), the CAS Key Technology Talent Program, China (173059000000160006), CAS Key Laboratory of Science and Technology on Operational Oceanography (OOST2021-02), Hainan Provincial Natural Science Foundation of China (421QN380), and Guangzhou Science and Technology Project, China (202102020464).

References

[1] Gunn K, Stockwilliams C. Quantifying the global wave power resource. Renew Energy 2012;44:296–304.
[2] Rusu E, Rusu L. An evaluation of the wave energy resources in the proximity of the wind farms operating in the north sea. Energy Rep 2021;7:19–27.
[3] Pérez-Collazo C, Greaves D, Iglesias G. A review of combined wave and offshore wind energy. Renew Sustain Energy Rev 2015;42:141–53.
[4] Zhang D, Li W, Lin Y. Wave energy in China: Current status and perspectives. Renew Energy 2009;34:2089–92.
[5] Hughes MG, Heap AD. National-scale wave energy resource assessment for Australia. Renew Energy 2010;35:1783–91.
[6] Li B, Chen W, Li J, Liu J, Shi P. Integrated monitoring and assessments of marine energy for a small uninhabited island. Energy Rep 2022;8:63–72.
[7] Morim J, Cartwright N, Etemad-Shahidi A, Strauss D, Hemer M. Wave energy resource assessment along the Southeast coast of Australia on the basis of a 31-year hindcast. Appl Energy 2016;184:276–97.
[8] Wang Z, Duan C, Dong S. Long-term wind and wave energy resource assessment in the South China sea based on 30-year hindcast data. Ocean Eng 2018;163:58–75.
[9] Sun Z, Zhang H, Xu D, Liu X, Ding J. Assessment of wave power in the South China sea based on 26-year high-resolution hindcast data. Energy 2020;197:117218.
[10] Sun Z, Zhang H, Liu X, Ding J, Cai Z. Wave energy assessment of the Xisha Group Islands zone for the period 2010–2019. Energy 2021;220:119721.
[11] Liang B, Shao Z, Wu G, Shao M, Sun J. New equations of wave energy assessment accounting for the water depth. Appl Energy 2017;188:130–9.
[12] Cavaleri L, Alves JHGM, Ardhuin F, Babanin A, Banner M, Belibassakis K, Benoit M, Donelan M, Groeneweg J, Herbers THC, Hwang P, Janssen PAEM, Janssen T, Lavrenov IV, Magne R, Monbaliu J, Onorato M, Polnikov V, Resio D, Rogers WE, Sheremet A, McKee Smith J, Tolman HL, van Vledder G, Wolf J, Young I. Wave modelling – The state of the art. Prog Oceanogr 2007;75:603–74.
[13] Chen X, Wang K, Zhang Z, Zeng Y, Zhang Y, O'Driscoll K. An assessment of wind and wave climate as potential sources of renewable energy in the nearshore Shenzhen coastal zone of the South China Sea. Energy 2017;134:789–801.
[14] Li B, Chen W, Liu J, Li J, Wang S, Xing H. Construction and application of nearshore hydrodynamic monitoring system for uninhabited islands. J Coast Res 2020;99:131–6.
[15] Chen W, Li J, Liu J, Li B, Shi P, Xing H, Long X. An integrated correction algorithm for multi-node data from the hydro-meteorological monitoring system in the South China Sea. Lecture Notes in Comput Sci 2021;12753:121–6.
[16] Zheng CW, Zhuang H, Li X, Li XQ. Wind energy and wave energy resources assessment in the east china sea and south china sea. Sci China Technol Sci 2012;55:163–73.
[17] Cornett AM. A global wave energy resource assessment. In: Proceedings of 18th International Conference on Offshore and Polar Engineering. BC, Canada, Vancouver: The International Society of Offshore and Polar Engineers; 2008.
[18] Wan Y, Fan C, Dai Y, Li L, Sun W, Zhou P, Qu X. Assessment of the joint development potential of wave and wind energy in the South China Sea. Energies 2018;11:1–26.
[19] Stopa JE, Filipot JF, Li N, Cheung KF, Chen YL, Vega L. Wave energy resources along the Hawaiian Island chain. Renew Energy 2013;55:305–21.
[20] Wan Y, Zhang J, Meng JM, Wang J. Exploitable wave energy assessment based on ERA-Interim reanalysis data — A case study in the East China Sea and the South China Sea. Acta Oceanol Sinica 2015;34:143–55.
[21] Sun J, Guan C, Liu B. Ocean wave diffraction in near-shore regions observed by Synthetic Aperture Radar. Chin J Oceanol Limnol 2006;24:48–56.
[22] Lentz SJ, Churchill JH, Davis KA, Farrar JT. Surface gravity wave transformation across a platform coral reef in the Red Sea. J Geophys Res Oceans 2016;121:693–705.

[23] Su H, Wei C, Jiang S, Li P, Zhai F. Revisiting the seasonal wave height variability in the South China Sea with merged satellite altimetry observations. Acta Oceanol Sinica 2017;36:38–50.
[24] Wang H, Fu D, Liu D, Xiao X, Liu B. Analysis and prediction of significant wave height in the Beibu Gulf, South China Sea. J Geophys Res Oceans 2021;126:e2020JC017144.
[25] Wyrtki K. Physical Oceanography of the Southeast Asian Waters: Scientific Results of Marine Investigations of the South China Sea and the Gulf of Thailand, Vol. 2. NAGA Rep., La Jolla, Calif: Scripps Inst. of Oceanogr.; 1961, p. 195.
[26] Chu PC, Qi Y, Chen Y, Shi P, Mao Q. South China sea wind-wave characteristics. Part I: Validation of wavewatch-III using TOPEX/Poseidon data. J Atmos Ocean Technol 2004;21:1718–33.
[27] Liang B, Fan F, Yin Z, Shi H, Lee D. Numerical modelling of the nearshore wave energy resources of Shandong peninsula, China. Renew Energy 2013;57:330–8.
[28] Kim G, Jeong WM, Lee KS, Jun K, Lee ME. Offshore and nearshore wave energy assessment around the Korean Peninsula. Energy 2011;36:1460–9.
[29] Iglesias G, Carballo R. Offshore and inshore wave energy assessment: Asturias (N Spain). Energy 2010;35:1964–72.